

# **DEVELOPMENT OF A SCALABLE THERMOMECHANICAL PROCESS (TMP) FOR THICK BAINITIC ARMOR STEEL**

Henry Chu, Thomas Lillo, Jeffrey  
Anderson, Thomas Zagula

August 2018



The INL is a U.S. Department of Energy National Laboratory  
operated by Battelle Energy Alliance

# **DEVELOPMENT OF A SCALABLE THERMOMECHANICAL PROCESS (TMP) FOR THICK BAINITIC ARMOR STEEL**

**Henry Chu, Thomas Lillo, Jeffrey Anderson, Thomas Zagula**

**August 2018**

**Idaho National Laboratory  
Idaho Falls, Idaho 83415**

**<http://www.inl.gov>**

**Prepared for the  
U.S. Department of Energy  
Office of Nuclear Energy, Office of Nuclear Energy, Office of Nuclear Energy, Office of  
Nuclear Energy, Office of Nuclear Energy, Office of Nuclear Energy  
Under DOE Idaho Operations Office  
Contract Unknown, Unknown, Unknown, Unknown, Unknown, Unknown**

## DEVELOPMENT OF A SCALABLE THERMOMECHANICAL PROCESS (TMP) FOR THICK BAINITIC ARMOR STEEL

Henry S. Chu, PhD  
Thomas M. Lillo, PhD  
Jeffrey A. Anderson  
Thomas A. Zagula  
Idaho National Laboratory  
Idaho Falls, ID

### ABSTRACT

*A bainite phase-based alloy and associated thermomechanical process were developed to produce (2.5 to over 5 cm) thick armor-grade steel with uniform through-thickness high hardness and strength. The alloy composition and the final-critical (austenite to bainite) isothermal transformation step were specifically designed to utilize a simple and versatile air-cool/quench method to keep a low upfront capital cost and to provide the ability to continuously control the cooling rate in real time, in order to produce maximum volume fraction of bainite phase, and promote uniformly distributed strength and hardness. Final thickness of 2.5 cm and 5.7 cm steel plates were fabricated for characterization, testing and evaluation and found to possess uniform through-thickness hardness between 53 to 55 HRC and dynamic compressive strength of up to 2 GPa.*

### INTRODUCTION

Many traditional armor steels such as high-hardness (HH) and rolled homogenous armor (RHA) have been around since the World War II era. The hardness and strength of these traditional armor steel alloys are derived from the martensitic phases resulting from rapid water-quench processing. As such, thick (>2.5 cm) sections with uniformly-distributed strength and hardness, which are required to mitigate more lethal heavy threats, are impractically expensive to process and manufacture.

One overlooked high-strength steel technology that has potential for armor applications is nano-structured bainitic steel alloy [1-5]. Properly heat treated bainitic steel alloy can possess a wide range of combinations of strength, hardness, reasonable

ductility, and toughness – all of which are dependent on the specific alloy composition and the final isothermal transformation process. This ability to balance traits through composition and processing into a more customizable armor steel is desirable for applications ranging from train rails to armor [6]. The exceptional properties of bainitic steels have been investigated for applications in the transportation industry to reduce the weight of vehicles via the flash processing method [7]. Despite the desirable economies of this method, it is not capable of producing sections thicker than a few millimeters. Even the isothermal bainite transformation technique has not been applied to very thick steel processing by anyone in industry or academia. For example, in the recent study by Han et al. [8] the specimens were a mere 15 mm thick.

There is no published data for bainitic steels compositionally-designed for thicknesses on the order of centimeters (or inches).

As such, the existing bainitic steels lack the ability to replace or append traditional armor steels such as RHA and HH. To surmount this obstacle, researchers at the Idaho National Laboratory (INL) have focused on developing new alloy compositions and associated TMP techniques to manufacture thick slabs of bainitic steels ranging in thickness from 2.5 cm to over 5 cm and with uniform through-thickness hardness.

The objective of this paper is to present the methodology used by INL researchers in selecting and designing the alloy composition as well as co-developing the critical isothermal transformation heat treatment process to fabricate thick bainitic steel plates with uniform hardness equivalent to much thinner high-hardness (HH) armor steel [9]. Material characterization and some other limited results are also given.

## METHODS

The alloy composition selection and the customized air cool/quench isothermal transformation method for heat treating thick bainitic armor plates was the primary development of this research. For comparison purposes, some of the final composition 5.7 cm thick plates were quenched and isothermally transformed via a conventional salt bath process.

### *Alloy Development and Selection*

The final alloy composition ranges were developed over several iterations. A “material by design approach” was also used where initial alloy compositions were screened primarily by generating Time–Temperature–Transformation (TTT) diagrams similar to that shown in Figure 1. Each TTT diagram was evaluated based on several criteria. First, the time from zero to the onset of the pearlite transformation had to be long enough to allow cooling path to avoid that region. Second, the amount of time for the onset of the bainite

transformation to begin had to be about the same order of magnitude as that for the pearlite transformation. Finally, the nucleation limited bainite start temperature, the growth limited bainite start temperature, and the martensite start temperature had to be sufficiently separated. The reason for the last requirement was to permit the cooling path to be guided into, and maintained within by closed loop control, the desired region with a sufficient margin for error to accommodate an active control method, calculation uncertainty, and the errors associated with actual phase boundary locations based on the relatively slow air cooling rate to the isothermal transformation temperature [10]. Note also that the regions defined by the bainite start temperatures were assumed to be equivalent to the upper and lower bainite transformation regions. The computer code used to generate these TTT diagrams was originally developed by Peet and Bhadeshia [11], and was selected due to its ready availability. While the approximate nature of the TTT diagram when used in this way is acknowledged, the results of the study indicate that any shifts of transformation temperature and time boundaries must necessarily have remained within the allowed margin of error.

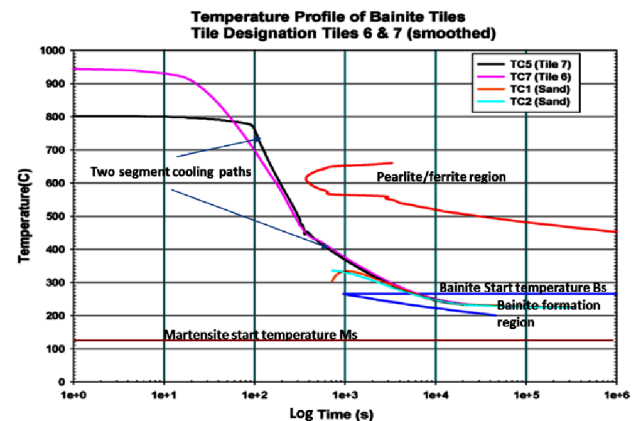


Figure 1: Typical TTT diagram used to determine the cooling rate(s) and path(s) to facilitate transformation of retained austenite to bainite. Composition (Wt %) used to generate this TTT diagram:

C	Si	Mn	Mo	Cr	Co	Al
0.72	1.80	1.93	0.26	1.60	0.12	0.75

Based on the information provided by the above-mentioned TTT diagram, in order for the critical isothermal transformation to occur effectively, it was determined that a multi-segments cooling process was needed. When each plate was removed from the high-temperature austenization furnace, the cooling had to be maintained at a relatively high rate in order to be safely below the “nose” of the pearlite region. On the other hand the cooling rate could not be too high resulting in an un-recoverable rapid quench to martensite start temperature,  $M_s$ , thus missing the isothermal transformation region of the bainite phase. In addition, a greatly reduced final cooling rate had the effect of reducing internal thermal gradients as the plate entered the bainite transformation, resulting in more uniform final properties.

For example, it can be observed from the TTT diagram depicted in Figure 1 that for the given composition, the first segment of the cooling path required a minimum cooling rate of  $3^\circ\text{C}/\text{sec}$  from an austenization temperature of  $950^\circ\text{C}$  in order for the plate temperature to safely drop below the pearlite transformation region. To achieve this critical cooling curve a process was devised to actively-control forced-air cooling while monitoring overall plate temperature and plotting it in real time over a TTT diagram template.

After avoiding the pearlite transformation, a slower cooling rate and path were used to “guide” the plate below the bainite start temperature,  $B_s$ , and into the isothermal transformation region as shown in Figure 1. Because of the long duration required to transform austenite to bainite (especially for a part with composition designed for thick cross-sections), the temperature of the plate had to be carefully controlled and automatically maintained. For this purpose, the plate was placed in a solid-particle thermal ballast to damp out temperature fluctuations during the long-duration unattended isothermal transformation. The thermal ballast was simply a stainless steel (SS) box situated inside an atmospheric furnace with a temperature setting at  $10^\circ\text{C}$  below bainite start temperature. The SS box was

filled with 90-grit pure alumina “sand” pre-heated to the same temperature setting. The alumina sands formed a 7 to 8 cm thick bed upon which the plate would be laid. Thermocouples used to monitor the first segment of the cooling curve remained embedded in the plate. After the temperature of the plate was confirmed to have reached  $10^\circ\text{C}$  below bainite start temperature, additionally pre-heated alumina sands were placed in the stainless steel box to encapsulate the plate completely with a 7-8 cm thick thermal ballast wall in all six sides. The temperatures of the plate were logged and monitored to ensure the plate remained inside the bainite transformation region for the pre-determined time duration. It was found that the uniquely designed solid-particle thermal ballast was able to maintain a stable temperature to within  $\pm 2^\circ\text{C}$  over 4 days with minimal periodic adjustment. Upon the completion of the designated bainite transformation step the plate was removed from the furnace and the SS box and allowed to cool to room temperature in a still-air ambient condition.

The research and development of the bainitic steel alloy composition and associated thermomechanical and isothermal transformation processes were performed in two experimental sequences. In the first (proof-of-concept) phase, a series of candidate compositions was analyzed iteratively based on their unique TTT diagrams as described previously. The composition-specific TTT diagrams furnished important information on the practicality of the cooling path and rate ( $^\circ\text{C}/\text{sec}$ ) required and cooling equipment needed to attain that rate.

To further assist the design of the cooling rate and path, and the associated cooling equipment, a thermal model was constructed to determine a-priori the thermal diffusion rate, whereby the temperature readings at several selected sites on the part could be used to determine inversely the approximate temperature at the core during actual cooling. This approach removed the need to drill holes into the center of the plate for insertion of thermocouples to directly monitor the plate core temperature and thus preserving the test plate for ballistic testing. A steel

plate of the same dimensions and composition with multiple Type-K thermocouples (TC) embedded was used to calibrate the thermal analytical model. The thermal analytical method described was further expanded and enhanced for the thermomechanical processing of much thicker (6 cm) bainite plate and the details are presented in a later section.

A final composition (Table 1) was selected for casting into billets, rolling, and machining into (2.5 x 10 x 10) cm test plates for development of the isothermal transformation process, phase characterization, mechanical property measurement, and ballistic evaluation. Tables 2 and 3 present the mechanical properties: hardness, hardness uniformity, static and dynamic strengths of the alloy.

**Table 1: Final composition (wt%) of 2.5 cm thick plates**

C	Si	Mn	Cr	Mo	Co	Al
0.72	1.80	1.93	1.60	0.26	0.12	0.80

**Table 2: Hardness (HRC) of 2.5 cm thick plates after 96 hours of isothermal transformation at constant 225°C**

Thru-thickness	Mean	53.8	Std dev	±0.24
Surface	Mean	54.4	Std dev	±0.52

**Table 3: Mechanical Properties of 2.5 cm thick plates**

0.2% YS, GPa	UTS, GPa	Elongation, %	Elastic Modulus, GPa	Dynamic UTS, GPa
1.545	2.041	4.74	201	2.25 @ 3560/sec

For ballistic property evaluation, the (2.5 x 10 x 10) cm test plates were tested against a 0.50 caliber APM2 with an aluminum witness plate placed behind each to measure residual depth of penetration (DOP). Residual penetration was gauged by the crater volume in the aluminum witness plate as measured with water-fill method. High-hardness armor steel (MIL-DTL-46100) of equal thickness (1.9 cm after surface preparation) was also tested by the same DOP method for comparison purposes. The DOP results are presented in Table 4, which shows the ballistic

properties of the two materials were statistically equivalent.

**Table 4: Ballistic property comparison using Depth of Penetration (DOP) tests.**

**Test rounds: 0.50 Caliber APM2. Impact velocity: 954 m/s**

Residual DOP Vol. (cc)				
1.9 cm bainite plate	Mean	1.99	Std dev	±1.24
1.9 cm High-Hard (Mil 46100)	Mean	1.73	Std dev	±1.02

After validation of the methodology developed to process 2.5 cm thick bainite armor steel the thermomechanical process was expanded and further enhanced in order to manufacture 6+ cm thick plates. Owing to the huge increase in thickness, and therefore the thermal mass, the enhancements focused on expanding the thermal model to include forced air cooling analysis as well as design and engineering of robust and flexible large-volume high-velocity air handling equipment in order to achieve the desired cooling curve.

### Scale Up and Final Alloy Processing

Billets of the composition shown in Table 1 were then cast to a size of (46 x 51 x 10) cm with a 5 cm radius nose along each of the 46 cm sides. During the casting process, several of the castings cracked either during the removal of the risers, or during subsequent shipment or processing. One billet that fractured into two pieces during the removal of the riser was analyzed to help determine the cause. The results showed that improper mixing of alloys and impure scrap additions were detrimental to the final casting quality. Improvements were implemented to produce castings of significantly better quality that were later successfully processed into bainitic steel plates with a much higher success rate. However, alloy element amount and mixing control remained somewhat inconsistent. Table 5 presents the range of as-received and specified chemical composition of twelve cast billets as measured by inductively coupled plasma atomic

emission spectroscopy (ICP-AES). As such it must be re-emphasized the importance of using composition-specific TTT diagram as a guide to design the cooling curve in order to maximize the formation of bainite phase in such thick plates.

**Table 5: Composition (in Wt%) of cast billets received**

	C	Si	Mn	M O	Cr	Al	Co	Ni	Cu
Specification	.69	1.92	2	.24	1.39	.75	.14	0	0
Min	.56	1.42	1.77	.2	1.39	.56	.15	.07	.07
Max	.8	1.86	1.91	.28	1.51	1.2	.22	.23	.08

The cast billets were homogenized in a nitrogen-atmosphere furnace at 1000 °C for 5 hours in an attempt to reduce intra-dendritic segregation of alloying elements. Each billet was later heated again and rolled to 6.4 cm thick plates. The final thickness after machining to remove a few minor surface cracks was about 5.7 cm thick. Each plate was subsequently divided into two equal ballistic target size pieces of about (38.1 x 45.7 x 5.7) cm for the final bainite transformation heat treatment.

To scale the process for the (38.1 x 45.7 x 5.7) cm plates, CFD and FEA methods were used to design a scalable, flexible, and inexpensive air cooled heat treatment process with associated apparatus to satisfy the requisite cooling rates and maximum allowable temperature gradients as estimated from each composition-specific TTT diagram. Figure 3 presents the results of a typical CFD and heat transfer analyses.

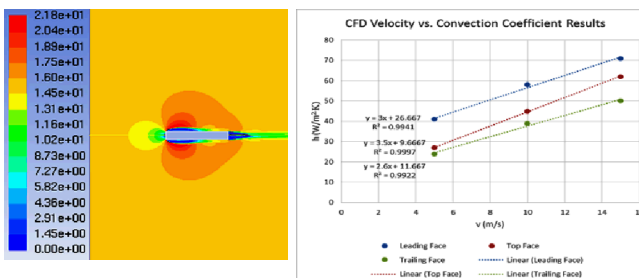


*Figure 3: Air flow velocity magnitude (m/s) contour plot showing flow over a 6.4:1 ratio rectangular plate calculated using ANSYS Fluent (LHS). Average heat transfer coefficients for each face of the CFD calculation (RHS).*

Figure 4 depicts a computed TTT diagram for one of the rolled (5.7 cm) thick plate (labelled as #4) and a cooling curve required to achieve the final austenite to bainite isothermal transformation.

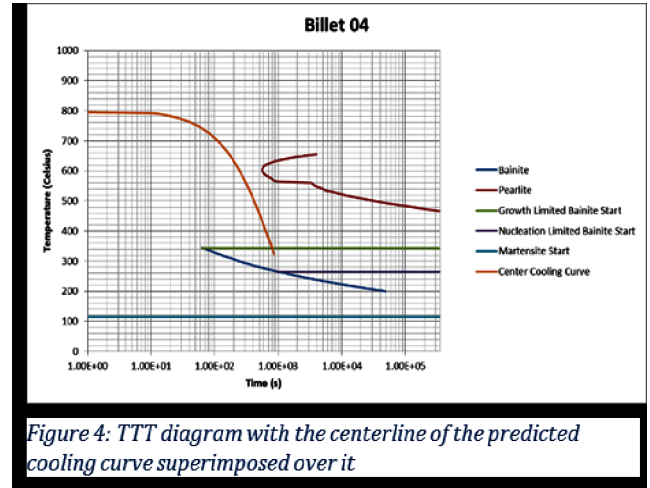


*Figure 4: TTT diagram with the centerline of the predicted cooling curve superimposed over it*

In order to achieve the required air velocities as calculated in the analysis and design study, a cooling rack/apparatus with air knives was designed and built as shown in Figure 5 with a 5.7 cm thick plate and removable furnace rack in place. A regulator was installed in the air line to meter the flow as necessary. The air knives were also removable and adjustable to facilitate placement and removal of plates of various sizes. Each plate was also instrumented with TC at three locations along the edges and surface. From the FEA model, the temperature difference between the edges, surface, and center were estimated and used to monitor and actively control the cooling process in real-time.



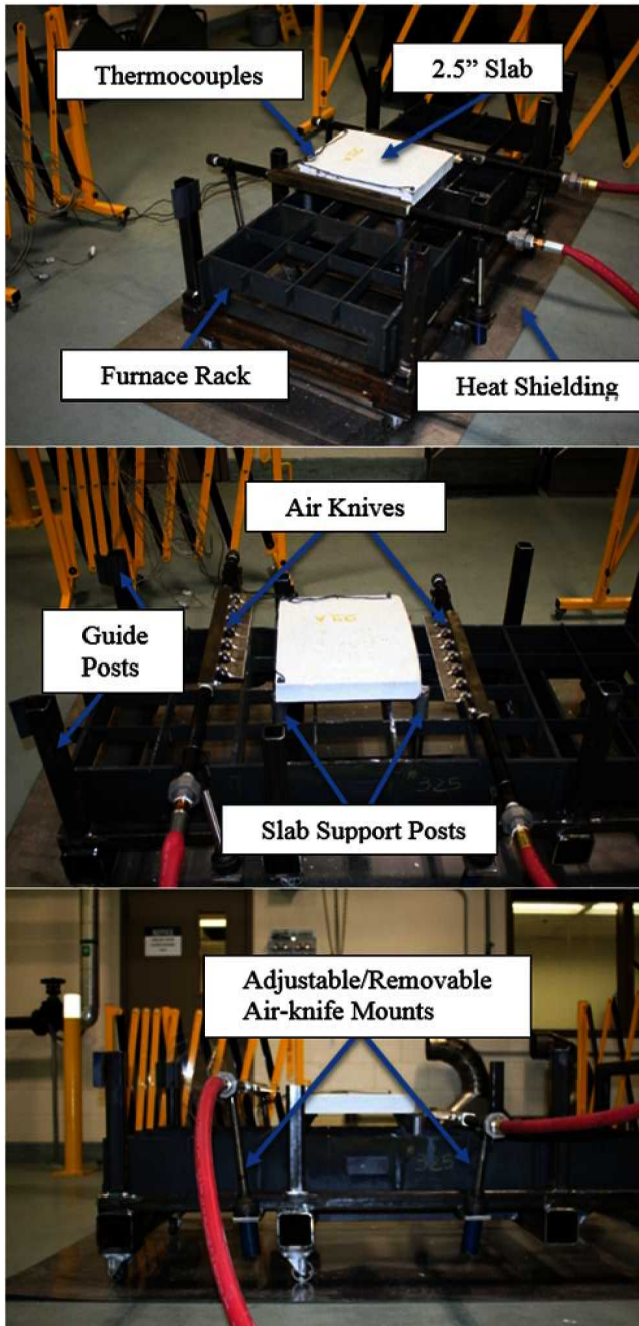


Figure 5: Forced air cooling apparatus for 5.7 cm thick plates.

Although the inexpensive air cooled process was the primary objective of this research, for the purpose of comparison, a nitrate-nitrite salt bath process was also used to quench several plates from

an austenization temperature of 860 °C that was held for 100 minutes and hold them at the desired bainite transformation temperature of 240 °C. The salt bath method has the advantage of being immune to over-quenching and has a high heat transfer coefficient in the range of 4500-16500 W/m<sup>2</sup>·K [12]. However, this method is not able to achieve a bimodal or other final grain size distribution as is suggested for good impact toughness by Hase et al. [13].

### Material Characterization

After both air and salt bath heat treatments were completed, material characterization was performed on samples extracted from the edges of each plate to preserve the rest of the plate for ballistic testing. The hardness was determined using a Rockwell Hardness indenter with 150 kilogram load on the Rockwell “C” scale. Samples extracted from various plates were mounted and polished for metallographic characterization. Polished samples were prepared using a 10% sodium metabisulfite etchant that caused bainite to appear blue under polarized light. A follow-on etching with 2-5% Nital caused the austenite/ferrite phase to appear white and martensite phase dark to dark-brown in the metallographic images. Figure 6 presents examples of color tint etched samples extracted from various plates heat treated by forced air and salt bath methods. Image analysis was performed in three randomly selected areas on each samples to determine the area fraction of bainite in each sample. Additionally, the amount of retained austenite was determined using x-ray diffraction according to ASTM E975-13: *Standard Practice for X-Ray Determination of Retained Austenite in Steel with Near Random Crystallographic Orientation*. The hardness and amount of retained austenite/bainite of the forced air and salt bath treated plates are presented in Table 6. Dynamic properties such as those presented in Table 3 for the 2.5 cm thick plates are being measured and will be reported in a future publication. To characterize the ballistic performance, a series of



V<sub>50</sub> tests were conducted with 30 mm L21A1 RARDEN APDS equivalent rounds on the heat-treated 5.7 cm thick plates. However, the ballistic results will only be presented in a restricted forum.

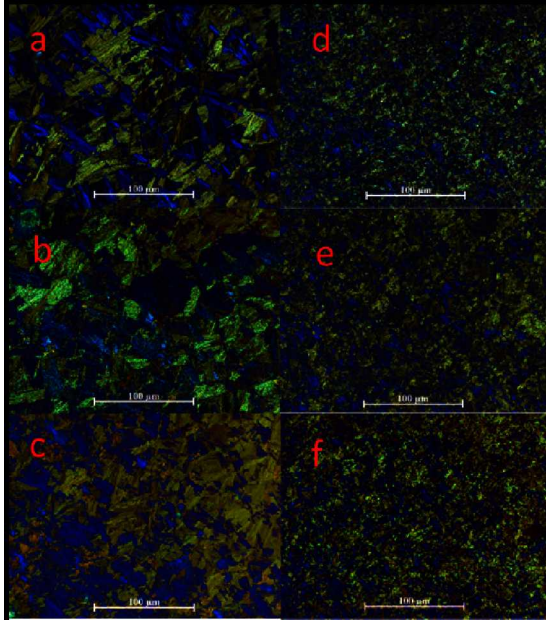


Figure 6: Bainite samples that have been tint etched for image analysis. (a) Sample 03A, (b) Sample 04A, (c) Sample 04A, 2<sup>nd</sup> try, (d) Sample 03B, (e) Sample 04B and (f) Sample 09B. Material in the left column ((a), (b), (c)) was processed with air while material in the right column ((d), (e), (f)) was processed in the salt bath.

Table 6: Tabulation of hardness and volume fraction of bainite formed

Sample ID	Hardness	Retained Austenite	Bainite fraction	
03B	50.0	10.54	22	Salt Bath
04B	54.3	8.93	28.1	
09B	54.6	9.9	24.5	
03A	44.9	18.8	18.3	Air Cool
04A	44.9	18.26	26.7	
04A-2nd time*	49.1	10.17	28.9	
09A	46.3	16.43	26.3	
11B	53.4	9.89	24.8	

## DISCUSSION

During actual cooling of the 5.7 cm thick plates, the cooling rate reached up to 2 °C/s during the initial stage and was asymptotically reduced as the bainite transformation temperature was approached. The isothermal transformation temperature was varied with composition for different plates within a range of 220 °C to 240 °C such that it fell between the nucleation limited bainite start and the martensite start temperatures as shown on the TTT diagram in Figure 4.

The initial 5.7 cm thick plate that was heat treated was not sufficiently cooled before placing it in the thermal ballast particles. As a consequence, the hot core raised the temperature of the plate significantly above the desired bainite transformation temperature for an extended period of time. Subsequent plates had the final cooling rate further reduced to permit better equalization of the plate temperatures before advancing to the isothermal transformation process.

Of the 5.7 cm plates, three were heat treated in a nitrate-nitrite salt bath and were designated as samples 3B, 4B and 9B. Samples from 4 plates were heat treated with a forced air quench and were designated as Samples 3A, 4A, 4A-2<sup>nd</sup> try, 9A and 11B (It was found after characterization that plate 4A was incorrectly heat treated due to the above mentioned core heating and this plate was re-heat treated. Samples from this re-heat treated plate were designated and subsequently reported as “4A-2<sup>nd</sup> try”).

The hardness and volume fraction of bainite phase data for the 5.7 cm thick plates from each sample was compiled and reported in Table 6 with the results for the salt bath and forced air quenched processed materials reported separately. Immediately noticeable is that the hardness of the salt bath quenched plates are consistently and significantly higher than those processed using the forced air quench for plates in the same series, e.g. 03B vs. 03A, where A and B denote the separate

halves of the same plate. Also, the salt bath processed plates have less retained austenite than the sister plate processed by air. However, the bainite fraction is not significantly different between the salt-processed and air-processed plates. The correlation between hardness and the retained austenite or bainite fraction is presented graphically in Figure 7.

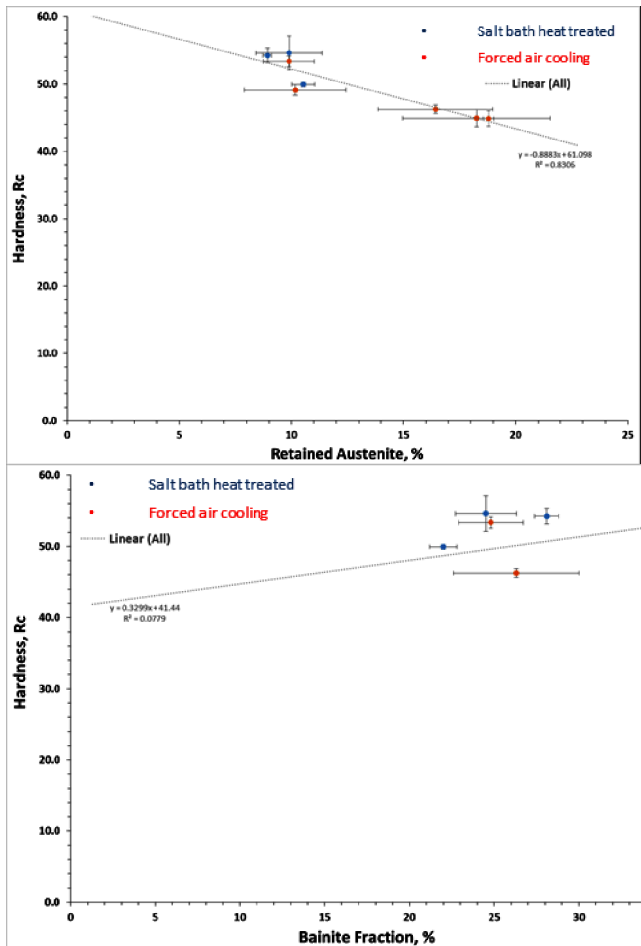


Figure 7: Relationship between hardness and the amount of retained austenite (Top) and hardness and bainite fraction (Bottom).

In this figure it is evident that the hardness correlates reasonably well with the amount of retained austenite. It must be kept in mind, however, that the composition of the steel is not strictly constant for the data in this plot. Therefore, with this caveat in mind, it would

appear that to increase hardness, the amount of retained austenite must be minimized. The amount of retained austenite can be minimized by maximizing the amount of bainite formed since austenite is decomposed to bainite during the isothermal phase transformation. Time, temperature, and steel composition can all affect the amount of bainite formed. However, there generally is either a practical limit, such as the length of the bainite transformation heat treatment, or a physical limit resulting from residual stress generation due to the bainite transformation that limits any further formation of additional bainite. The remaining austenite may then transform to martensite upon cooling below the martensite start temperature. (Here, again, the amount of martensite that can be formed, and thus the final amount of retained austenite, is limited by residual stresses caused by the martensite transformation and also can be affected by the steel composition). It may well be that the steels with lower retained austenite fractions formed more martensite which resulted in the higher hardness.

One notable observation not quantified in this summary is the size of the bainite colonies. Figure 6 shows representative microstructures from each series. Oddly, the size of the bainite colonies is dependent on the method used to quench from the austenitization temperature to the bainite transformation temperature. The bainite colonies of material processed by air quench were always larger than sister plates processed via salt bath method. The difference is also very large in all cases. The dissimilarity in size may be the cause of the difference in hardness between material processed by salt bath versus sister material processed by air even though the fractions of bainite are approximately the same for each material. Generally, microstructural features that are on a finer scale typically result in higher strength and hardness which seems to be the case here. Conversely, larger bainite colonies can be expected to exhibit better ductility, based on

standard metallurgical principles which imply a tradeoff between higher strength at the expense of lower ductility and vice versa. The optimal balance of these properties depends on the specific threat and application that the armor is being designed for, e.g. harder plates perform better against kinetic energy projectiles while tougher material works better for protection from blast fragments [14].

The scale of microstructural features is generally determined by temperature. In this case the material processed by air quench had a slower cooling rate in the regime where bainite started to form on its way to the isothermal transformation temperature as illustrated in Figure 10. The actual salt bath cooling curve is unknown because the salt bath equipment used in this research prevented insertion and attachment of thermocouples, but it undoubtedly resulted in much more rapid cooling rate as depicted. Since the bainite in the air cooled plates would have begun to nucleate and grow at a higher temperature than that formed during the salt bath quench, it follows that the slower multi-stage cooling path was the primary cause of the difference in grain morphologies.

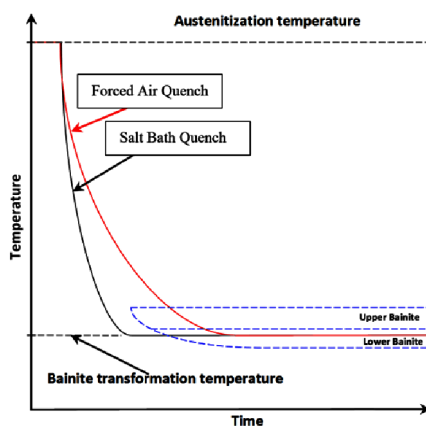


*Figure 10: Notional schematic representation of the cooling behavior experienced by material processed by salt and air. The forced-air cooling rate to the isothermal bainite transformation temperature may have traversed the upper bainite region of the time-transformation diagram.*

## CONCLUSIONS

The cooling path has proven to be the most critical process control feature for influencing final material properties for thick bainitic steels. Rapid salt bath quenching results in a finer, harder, but more brittle grain structure. Conversely, the controlled air cooling led to a courser and less brittle microstructure with a virtually infinite range of possibilities for process optimization.

The approach outlined here offers the potential for successful processing of very thick ( $> 2.5$  cm) bainitic steel plates by tailoring the composition and thermomechanical process to achieve the proper balance of mechanical and ballistic properties relevant to armor application. The air quench process has proven to be flexible, versatile and inexpensive to implement. This would also suggest that the capital equipment investment for future large scale production of bainitic steel plates or articles with arbitrary thick cross-sections would be relatively low compared to water or salt bath quench methods. However, a significant amount of work remains to optimize and automate the process.

## ACKNOWLEDGEMENTS

The authors would like to acknowledge the support of this effort provided by the DOE LDRD SM101 Project and a Memorandum of Agreement between the Idaho National Laboratory and Tank Automotive Research, Development and Engineering Center (TARDEC).

## REFERENCES

- [1] C. Garcia-Mateo, F. G. Caballero and H. K. Bhadeshia, "Development of Hard Bainite," *ISIJ International*, vol. 43, no. 8, pp. 1238-1243, 2003.

- [2] H. K. Bhadeshia, "Hard Bainite," *Solid Phase Transformations in Inorganic Materials*, vol. 1, pp. 469-484, 2005.
- [3] H. K. Bhadeshia, "Bainitic Bulk-Nanocrystalline Steel," in *The 3rd International Conference on Advanced Structural Steels*, Pohang Korea, 2006.
- [4] H. K. Bhadeshia, "Nanostructured Bainite," *Proc. R. Soc.*, vol. 466, pp. 3-18, 2010.
- [5] Y. Han, H. Wu, C. Liu and Y. Liu, "Microstructures and Mechanical Characteristics of a Medium Carbon Super-Bainitic Steel After Isothermal Transformation," *ASM International*, vol. 23, pp. 4230-4236, 2014.
- [6] H. K. Bhadeshia, "High Performance Bainitic Steels," *Materials Science Forum*, Vols. 500-501, pp. 63-74, 2005.
- [7] T. Lolla, G. Cola, B. Narayanan, B. Alexandrov and S. S. Babu, "Development of Rapid Heating and Cooling (Flash Processing) Process to Produce Advanced High Strength Steel Microstructures," *Materials Science and Technology*, vol. 27, no. 5, pp. 863-875, 2011.
- [8] Y. Han, W. Xiu, C. Liu and H. Wu, "Isothermal Transformation of a Commercial Super-Bainitic Steel: Part 1 Microstructural Characterization and Hardness," *Journal of Materials Engineering and Performance*, vol. 26, pp. 472-477, 2017.
- [9] A. R. Laboratory, "MIL-DTL-46100," 2015.
- [10] J.-C. Zhao and M. R. Notis, "Continuous Cooling Transformation Kinetics Versus Isothermal Transformation Kinetics of Steels: A phenomenological Rationalization of Experimental Observations," *Materials Science and Engineering*, vol. R15, pp. 135-208, 1995.
- [11] M. Peet and H. K. Bhadeshia, "Materials Algorithms Project," [Online]. Available: <https://www.phase-trans.msm.cam.ac.uk/map/steel/programs/mucg83.html>. [Accessed 7 March 2016].
- [12] G. P. Dubal, "Salt Bath Quenching," *Advanced Materials and Processes*, vol. 156, no. 6, pp. H23-H28, 1999.
- [13] K. Hase, C. Garcia-Mateo and H. K. Bhadeshia, "Bimodal Size-Distribution of Bainite Plates," *Materials Science and Engineering A*, Vols. 438-440, pp. 145-148, 2006.
- [14] J. Prifti, M. Castro, R. Squillacioti and R. Cellitti, "Improved Rolled Homogeneous Armor (IRHA) Steel Through Higher Hardness," ARL, Adelphi, 1997.